# Testing a new grain-size dependent isochron cosmogenic nuclide burial dating method: Eastern Cordillera, Colombian Andes

Sean Des Roches

Submitted in Partial Fulfilment of the Requirements for the
Degree of Bachelor of Science, Honours
Department of Earth Sciences
Dalhousie University, Halifax, Nova Scotia
March 2015

# Distribution License

DalSpace requires agreement to this non-exclusive distribution license before your item can appear on DalSpace.

NON-EXCLUSIVE DISTRIBUTION LICENSE

You (the author(s) or copyright owner) grant to Dalhousie University the non-exclusive right to reproduce and distribute your submission worldwide in any medium.

You agree that Dalhousie University may, without changing the content, reformat the submission for the purpose of preservation.

You also agree that Dalhousie University may keep more than one copy of this submission for purposes of security, back-up and preservation.

You agree that the submission is your original work, and that you have the right to grant the rights contained in this license. You also agree that your submission does not, to the best of your knowledge, infringe upon anyone's copyright.

If the submission contains material for which you do not hold copyright, you agree that you have obtained the unrestricted permission of the copyright owner to grant Dalhousie University the rights required by this license, and that such third-party owned material is clearly identified and acknowledged within the text or content of the submission.

If the submission is based upon work that has been sponsored or supported by an agency or organization other than Dalhousie University, you assert that you have fulfilled any right of review or other obligations required by such contract or agreement.

Dalhousie University will clearly identify your name(s) as the author(s) or owner(s) of the submission, and will not make any alteration to the content of the files that you have submitted.

If you have questions regarding this license please contact the repository manager at dalspace@dal.ca.

Grant the distribution license by signing and dating below.

_____ _____

Name of signatory Date

## Abstract

Terrestrial cosmogenic nuclide burial dating a powerful tool by which one can determine the timing of the burial of a layer of sediment or rock. A recently developed $^{26}Al/^{10}Be$ isochron burial dating approach uses samples with differing TCN concentrations collected from depth profiles in buried sediment. However, the use of this isochron burial dating method is dependent on finding a buried paleosol, or any surface that was exposed for a sufficient period of time (depending on duration of decay during burial) and then subsequently buried. In regions of high relief, which are prone to landslides, there may be an alternative methodology for isochron burial dating of sediments lacking paleosols. We evaluate here a new method of $^{26}Al/^{10}Be$ isochron burial dating based on the previously observed relationship between fluvial sediment grain size and TCN concentration in landslide-prone catchments. There may be a sufficient range in TCN concentration across the different grain sizes (150 to 2000 um) that an isochron curve can be precisely defined.

Fine sand to granular gravel fractions were extracted from five 3 kg sediment samples previously collected 112 m below an incised river terrace in the Eastern Cordillera of the Colombian Andes (4.979 N, 72.825 W, 686 m elevation above sea level). This site is ideal to test the new technique because its ongoing tectonic activity has generated high relief, landslides, and high erosion rates (therefore low TCN concentrations to test the method's limit).

Pure quartz from six different grain size fractions was extracted, cleaned, dissolved, and converted to $Al_2O_3$ and BeO AMS targets at the Dalhousie Geochronology Center. Calculations of the results from the AMS (Accelerator Mass Spectrometer) at Lawrence Livermore National Lab gave $^{26}Al$ concentrations ranging from 2.79 to 4.19 X $10^4$ atoms/g (±21% 1-sigma) and $^{10}Be$ concentrations ranging from 4.08 to 8.14 X $10^3$ (±4-8% 1-sigma) across various grain-size fractions. The measured values were too low and had too little variation to be able to define an isochron. With these results we were not able to test the effectiveness of a grain-size dependent isochron method.

We attribute the low measured AMS values in part to low initial TCN concentrations, which are the result of rapid erosion in the catchment area where the samples originated. Aluminum and beryllium may have also been lost during steps within the chemical preparation of the samples owing to the much larger quartz masses used than usual and to additional chemical isolation procedures that were used on the samples. Calculated paleo-erosion rates confirm high erosion rates for the catchment, which are 2.59 mm $yr^{-1}$ (±25% 1-sigma) based on $^{10}Be$ and 0.97 mm $yr^{-1}$ (±33% 1-sigma) based on $^{26}Al$, which are consistent with other rapidly eroding tectonically active orogens.


**Key Words**: Cosmogenic Isochron Grain-Size Beryllium Aluminum Andes Colombia

**Table of Contents**

## List of Figures



## List of Tables

**Acknowledgments**

First I would like to thank John Gosse for all of the guidance and support he provided over the course of my thesis. His enthusiasm and positive attitude kept me hard at work even at the most difficult of times. I have learned so much from him during our weekly meetings (and not just about my thesis).

I need to thank Guang Yang for all of her help with the chemistry. Her tutelage in the lab was invaluable, and without her help this thesis could never have been finished on time.

Thanks to Martin Gibling for all of his help in preparing my thesis and keeping me on tract. Also thanks to Mike Taylor and Gabriel Veloza Fajardo who did the hard work by going to Columbia and collecting the samples. Thanks to Alan Hidy and Susan Zimmerman who managed to get great AMS measurements from my difficult samples.

And of course many thanks to all of my friends and family, who provided invaluable support. The fact that they took the time to try and understand cosmogenic isotopes so that they could listen to me talk about about my thesis meant a lot.

## 1.0 Introduction

Terrestrial cosmogenic nuclide (TCN) burial dating is a powerful tool used in many different situations to develop a better understanding of the geology of a region. This thesis will focus on the $^{26}Al/^{10}Be$ system in quartz. This burial dating method has a wide range of applications and has been used to date alluvial fan surfaces, terraces and lava flows, to name a few examples (Granger & Muzikar, 2001). Burial dating has also been used to date strain markers, which can be used to determine the deformation history and develop a tectonic interpretation for a region (Gosse & Phillips, 2001).

The strength of TCN burial dating is that it can be used where other methods cannot. For sediments older than 50 ka and 1.5 Ma, respectively, radiocarbon and luminescence dating are not viable (Blaco & Rovey, 2008). Sediments of Pliocene-Pleistocene age can be dated with U-series or tephrochronology only in rare instances where suitable material is available in a useful stratigraphic sequence (Balco & Rovey, 2010). While there are limitations to the application of TCN burial dating, the technique can be used on a variety of different isotope-mineral systems (e.g. $^{26}Al$ and $^{10}Be$ in quartz) and a broad age range from $10^3$ years with a short-lived isotope, to $10^7$ years with a long lived isotope (Gosse & Phillips, 2001).

The most significant weakness of cosmogenic burial dating is that an assumption about the value of the initial $^{26}Al/^{10}Be$ ratio for a sample must be made (Hidy, 2013). In order to calculate an age, the initial ratio of $^{26}Al$ to $^{10}Be$ must be known (Balco & Rovey, 2010). This is very difficult where sediment is involved. Sediment, which has been eroded from a source, has an unknown inheritance of $^{26}Al$

and $^{10}$Be (Balco & Rovey, 2010). It is impossible to measure the initial ratio of $^{26}$Al /$^{10}$Be in these situations so an assumption is made that the initial ratio of $^{26}$Al /$^{10}$Be in the sediment is equal to the surface production ratio for $^{26}$Al /$^{10}$Be of 6.75 (Balco & Rovey, 2008).

A TCN isochron burial dating method was first employed by Balco & Rovey, (2008) to reduce the sensitivity of a burial age to the initial isotopic ratio. Application of the isochron burial dating method requires samples from a depth profile in the soil of a sediment package that was exposed prior to burial. If exposure was sufficiently long (many thousands of years) significant in-situ production of TCN in the quartz sand would have rendered any initial $^{10}$Be or $^{26}$Al inconsequential (Balco & Rovey, 2008). The isochron of interest is the slope of the ratio of two isotopic concentrations. The slope of $^{26}$Al /$^{10}$Be isochron (which is actually a curve owing to the fact that their production rates and decay rates are different) is best defined if there is a significant range of $^{26}$Al and $^{10}$Be among different samples at the site. Such a range can be achieved by analyzing multiple samples in a depth profile, because the cosmic rays are absorbed as they interact with mass. Thus, the samples near the top of a buried profile can have an order of magnitude higher concentrations than those at the bottom (Balco & Rovey, 2008). However, this variation of $^{26}$Al and $^{10}$Be concentration with depth only develops when the surface has been exposed for a long enough period of time (Balco & Rovey, 2010). Sampling is often done within paleosols as these are indicative of surfaces that have experienced a long period of exposure.

There is another option for sampling related samples with a range of $^{26}Al$ and $^{10}Be$ concentrations. In locations where cobbles are present it is possible that the concentration of $^{26}Al$ and $^{10}Be$ in each cobble would be sufficiently different (i.e. if they were exhumed from different depths just prior to deposition) to define an isochron. This experiment has been recently conducted and shown that the scatter is sufficient (Balco et al., 2013).

However, in many locations there are no paleosols to sample for burial dating of sediments or the fluvial sediments are sufficiently fine grained that no cobbles are present (e.g. on coastal plains such as the Pliocene Beaufort Fm at Beaver Pond Site, Ellesmere Island, Canada; Rybczynski et al, 2013). In such cases, a different method is needed for cosmogenic burial dating. This thesis proposes one such method.

The measurement of TCN in different grain size fractions in sediment from steeply sloped catchments, which are prone to landslide, should provide sufficient range in the TCN concentrations to define an isochron. This strategy makes use of the fact that depth profiles exist in catchments, and that mass wasting events can sample them, as opposed to surface runoff which would just sample the uppermost regolith-bearing sediment with more uniform concentrations of TCN. The upper part of the surface has been more weathered so it will break up into finer grained sediment, while deeper material will remain coarser grained.

The upper part of the surface was also exposed to more cosmic rays, so it will have higher concentrations of cosmogenic nuclides than the deeper sediment. It may be possible to use this nuclide concentration covariance with grain size instead

of a depth profile in the isochron dating method, eliminating the need to find a paleosol. In order to properly sample these profiles we would need the landslides to go to a mass depth of 1 $m/g^2$ below the surface.

Many previous studies have documented a TCN concentration variation with grain size while studying erosion rates for Pliocene and early Quaternary sediments in active orogens (Atinao, 2008; Belmont, 2007; Brown et al., 1996; Puchol et al., 2014; Veloza et al., unpub.). These studies were done in regions of high relief and it is believed this phenomenon can be attributed to the effect of deep-seated land sliding (Brown et al, 1996).

However, regions of high relief often have very rapid erosion rates, in part because of the landsliding and other accelerated hillslope processes. Increased erosion results in a decrease in the concentration of cosmogenic isotopes in sediment due to the deeper, lesser-exposed sediment being brought to surface. Therefore this thesis also proposes the idea that a grain-size dependent isochron method will not be able to be resolved, due to the decreased TCN concentrations resulting from rapid erosion in the catchment of high relief areas.

To reiterate, in this thesis two hypotheses will be tested: (H1) That the isochron method can be done using different grain size fractions, in regions prone to shallow landsliding and alternatively, (H2) that the high erosion rates associated with the catchments of regions with high relief will result in a decrease of TCN concentrations to the point where it will not be possible to get accurate enough measurements to define an isochron.

In this thesis the theory behind the grain-size dependent isochron method will be presented and a field test will be applied in the Tauramena locality of the Colombian Andes. This location is an ideal test site because (i) preliminary ages have already been done using a $^{26}Al$ /$^{10}Be$ simple burial dating method indicate minimum ages of 2.5 Ma (Veloza et al., unpub), which gives us an idea of what to expect; (ii) the Guayabo Fm comprises alluvial fan and fluvial terrace deposits at the mountain front of a high relief tectonically active origin where small landslides are common; (iii) a grain-size dependence has already been revealed in the Cordillera Principal of the Southern Central Andes (Antinao, 2008), suggesting that the same relationship may exist in the Colombian Andes; and (iv) the exact timing of the Guayabo Fm. is of significance because it may record a significant change in sediment flux at the Plio-Pleistocene boundary (2.6 Ma).

If this method proves functional, then it can be applied to other terrains with steep slopes where landslides or other mass wasting processes occur, which cause the erosion and deposition of subsurface regolith. For example Puchol et al. (2014) studied this phenomenon in a drainage basin in the central Himalayas and Belmont et al. (2007) noted this in Washington State.

## 2.0 Background and geologic setting

### 2.1 TCN dating principles

TCN methods use the production of particular nuclides in minerals from interactions of their atoms with cosmic rays (Granger & Muzikar, 2001). Cosmic rays are particles such as protons and muons that come from space and enter our atmosphere. TCN dating exclusively considers particles that originate outside of our solar system and which form primarily during supernova events (Gosse & Phillips, 2001). The flux of these particles to Earth is considered constant over the time periods for which TCN dating can be applied. However, the flux that reaches the surface of the Earth is altered significantly by the strength of the magnetic field, which varies spatially and temporally (Gosse & Phillips, 2001).

Interactions of cosmic rays with atoms in the atmosphere result in the production of secondary particles. These new particles may then collide with other atoms, creating more particles, resulting in a cascade effect, or cosmic ray shower. After an average of ten disintegrations, the secondary particles eventually make it to the surface of the Earth where they interact with atoms in minerals to create new nuclides (Granger & Muzikar, 2001). The depth to which the particles penetrate depends on their probability of interaction (or nuclear cross section), which is mainly a function of their energy, size, and charge (Gosse & Phillips 2001).

Many different nuclides are created, some of which are useful for geochronology and erosion rate applications, depending on decay rates and the

abundance of the isotopes produced by non-cosmogenic pathways (radiogenic or nucleogenic). For example $^{26}Al$ and $^{10}Be$, which are formed primarily by spallation, and have relatively small non-cosmogenic abundances, are both useful nuclides for calculating ages through the Pleistocene (Gosse & Phillips, 2001). $^{26}Al$ and $^{10}Be$ have half-lives of 0.705 Ma and 1.39 Ma, respectively (Balco & Rovey, 2011).

*Surface exposure dating*

TNC are commonly used to determine how long a surface has been exposed above ground (Gosse & Phillips, 2001). $^{26}Al$ and $^{10}Be$ nuclides are ideal for this method because they are both relatively immobile, form in quartz (which is the most abundant mineral in the continental crust), and have different half-lives and production rates (Gosse & Phillips, 2001).

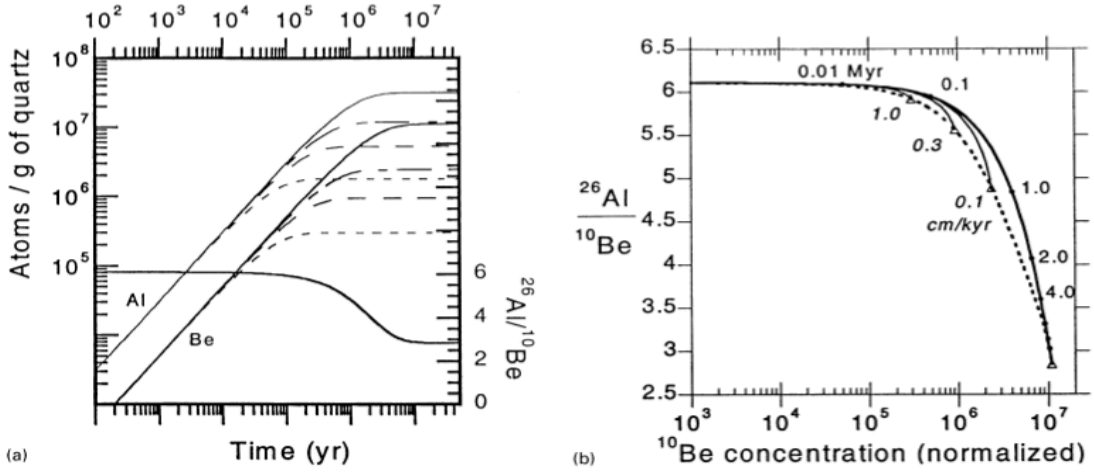


**Figure 1:** The production of $^{10}Be$ and $^{26}Al$ in quartz at sea level and high latitude by spallation and muon interactions.
**A.** Plot showing the build up of $^{26}Al$ and $^{10}Be$ in quartz over time. $^{26}Al$ is produced from $^{28}Si$ at a faster rate (higher cross section) than $^{10}Be$ from $^{16}O$ and $^{28}Si$ combined. Both nuclides eventually reach saturation, however the shorter-lived $^{26}Al$ reaches this point first. The dashed lines show how erosion rates of 0.1, 0.3, and 1.0 cm/kyr lower the concentration measured in the surface, and accelerate the saturation of each radionuclide. The bolded solid line shows the change in the $^{26}Al/^{10}Be$ ratio with time. These are based on production rates and decay constants that were used in 2001. Since then there have been updates to both.
**B.** A $^{26}Al$ /$^{10}Be$ vs. $^{10}Be$ plot (the zero-erosion scenario is represented by the thick, solid line). The thin lines with triangles show how the ratio of $^{26}Al$ /$^{10}Be$ would be affected by a given erosion rate. Samples that plot on the solid thick line provide an exact exposure age using both nuclides, and there is no indication of burial or erosion of the surface. Samples that plot in the banana-shaped field represent surfaces that have been exposed and eroded. Samples plotting below the banana indicate that the surface was exposed, and then completely or partially buried at least once (production was slowed or halted but decay continued, so the ratio decreased by an amount proportional with the burial duration). Figure from Gosse & Phillips, 2001.

The idea behind surface exposure dating is that as long as a surface is exposed it will be bombarded by cosmic rays and TCN will be produced. $^{26}Al$ is produced more quickly than $^{10}Be$, however the exact production rates vary depending on several factors such as latitude, altitude and shielding (Gosse & Phillips, 2001). The longer the surface is exposed the higher the concentration of TCN. Both of these radionuclides decay so eventually they will reach a saturation point, where production rate is equal to decay rate and their concentrations remain constant in the rock (Gosse & Phillips, 2001). $^{26}Al$ has a higher production rate and shorter half-life so it reaches its saturation point before $^{10}Be$, as shown in Figure 1a.

Due to the characteristics of these nuclides, their ratio changes significantly with time, as represented by the bold line in Figure 1b. Erosion of the surface will result in a decrease in the concentrations of $^{26}Al$ and $^{10}Be$, since erosion will advect previously partly shielded minerals toward the surface. The thinner lines with triangles in Figure 1b represent the effect of variable erosion rates on the ratio of $^{26}Al$ /$^{10}Be$. Surface exposure dating can be applied to surfaces of bedrock landforms (e.g. fault scarp, lava, or tor) or sediment landforms (e.g. terrace, fan, landslide).

*Simple burial dating.*

It is often useful to determine when a buried surface, such as a buried soil or peat, became shielded by other sediment, lava, or even water. This can be done with TCN burial dating. The ideal situation for this method is when the surface of interest was exposed for a long time (>$10^3$ years) and then is instantaneously buried, resulting in a complete stop in the flux of cosmic rays to the surface (Lal, 1991). In

other words, after burial there is no more production of cosmogenic nuclides but the $^{26}Al/^{10}Be$ ratio continues to decrease owing to differences in the decay rates of the isotopes (Fig. 1a,b). The decrease is proportional with burial time. If only one complete burial event has occurred, then the exact burial duration can be calculated (shown graphically in Fig. 2). In reality however, the situation is rarely ideal with complexities that must be taken into account, such as slow burial, re-exposure of the surface, and production of nuclides by deep-penetrating muons (Granger & Muzikar, 2001). To simplify calculations certain assumptions have to be made.

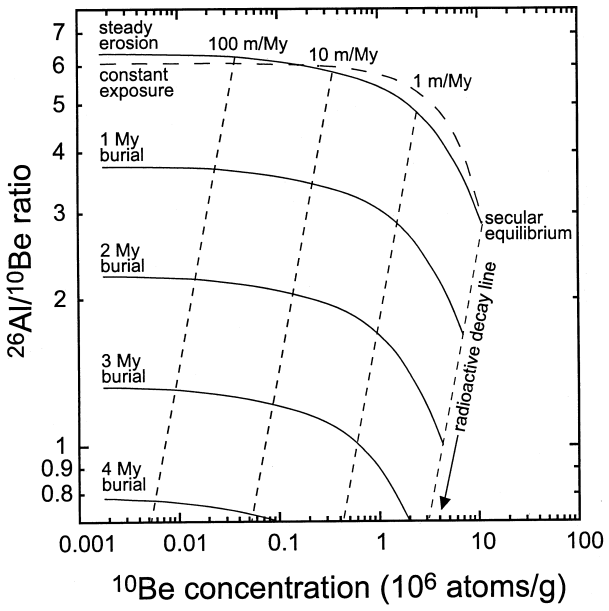


**Figure 2**: Burial plot for $^{26}Al/^{10}Be$. It represents the $^{26}Al/^{10}Be$ ratio in sediment over time. The topmost dashed line represents the change in the $^{26}Al/^{10}Be$ ratio in a surface with constant exposure (equivalent to the solid thick line of Fig. 1b). The topmost solid line represents the exposure time of a surface undergoing a range of steady erosion (as indicated by the dashed lines) but no burial. As soon as burial occurs, radioactive decay will control the $^{26}Al/^{10}Be$ ratio. The $^{26}Al$ and $^{10}Be$ ratios indicate burial duration, as indicated by the other solid curves which correspond to longer and longer burial age with decreasing ratio. Production rates and decay constants are as per 2001. Figure from Granger & Muzikar, 2001.

Since the half-lives of $^{26}Al$ and $^{10}Be$ are known, as is their production ratio, it is possible for us calculate how the ratio of $^{26}Al/^{10}Be$ would change through time in a buried surface. A burial duration is computed for a measured $^{26}Al/^{10}Be$ ratio (Fig. 2; Granger & Muzikar, 2001).

The simple burial dating method requires the assumptions that (i) the initial ratio of $^{26}Al/^{10}Be$ was 6.75 (i.e. that there was only one burial event and, in the case

of dating sediments, there was no prolonged sediment storage prior to the final deposition of the sediment) and (ii) that there was no post-burial muonic production. In other words, it was assumed that a single simple burial occurred. This assumption is the biggest weakness of TCN burial dating (Hidy, 2013).

The model for burial dating is that of a surface in a catchment area building up $^{26}Al$ and $^{10}Be$ at a ratio of 6.75 $^{26}Al$ atoms for every $^{10}Be$ atom (the production ratio was 6.1 in 2001, Fig. 1a,b; Fig. 2), and then the surface being eroded and immediately buried. If buried sediment in the real world does not actually follow this model, our assumption of the initial ratio of 6.75 is incorrect. If the ratio at the time of deposition was less, then the simple burial age will over-estimate the actual duration of the last burial event. In reality, by using the simple burial dating method we are calculating a maximum burial age (Balco & Rovey, 2010).

*Depth profile isochron method.*

To resolve this issue, isochron burial dating was developed. The premise of this method is to avoid the assumption of an initial ratio of 6.75 by sampling in a manner that circumvents the need to make the assumption (Balco & Rovey, 2008). This can be done by taking a depth profile below a previously exposed surface. It is well documented that TCN concentrations decrease with depth (Lal, 1991). Sediment at a landforms surface will have the maximum production of nuclides for a particular layer. As depth increases, the sediment at depth becomes more shielded by the sediment above. Fewer cosmic rays are able to penetrate to depth due to their interactions with the sediment at surface.

This attenuation of the cosmic ray energy is predictable based on knowledge of the secondary cosmic ray flux (particle energy, type) and nuclear cross sections for their interactions with target minerals. This phenomenon is illustrated in Figure 3, below. Though the concentrations of $^{26}Al$ and $^{10}Be$ vary with depth through a layer of sediment, the ratio of $^{26}Al/^{10}Be$ should be the same (at least in the upper 2 meters) through the entire sediment package since the total cosmic ray flux to the sediment package was the same (Balco & Rovey, 2008). At greater depth, the greater production of $^{26}Al$ than $^{10}Be$ by muons will change the ratio. So, by sampling within the first 2 meters of a buried soil (200 cm in a sediment with bulk density of 2 g $cm^{-3}$ is equivalent to a mass depth of 400 g $cm^{-2}$, Fig. 3) a constant isochron can be defined, whereby the slope of the $^{26}Al$ /$^{10}Be$ curve is a function of burial duration (Fig. 4).

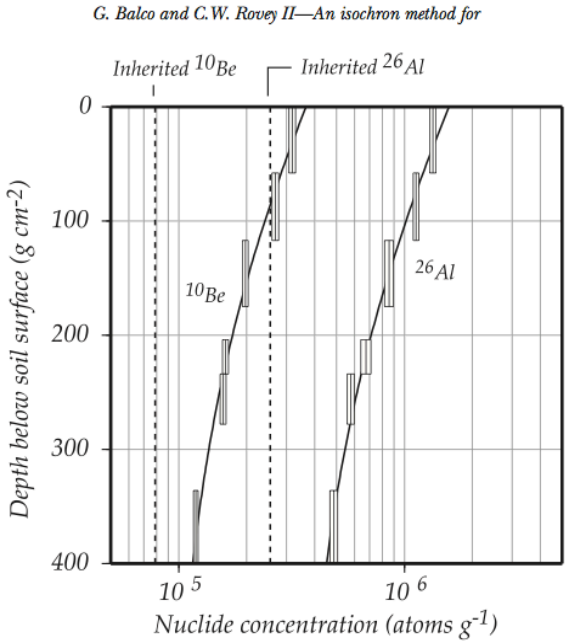


**Figure 3**: Measured $^{26}Al$ and $^{10}Be$ concentrations below a paleosol. There is a clear decrease in concentration with depth, however the ratio of $^{26}Al$ and $^{10}Be$ remains the same. Note the y-axis is mass depth, a function of true depth and bulk density. Figure from Balco & Rovey, 2008.

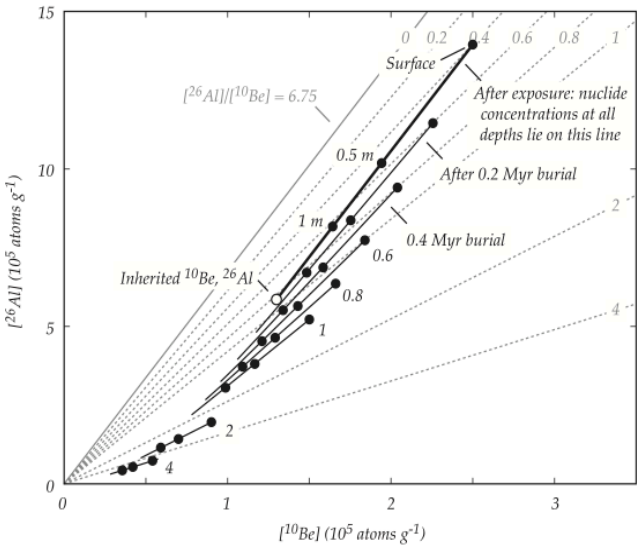


**Figure 4**: An isochron burial plot. $^{26}Al$ and $^{10}Be$ concentrations in quartz are plotted against each other. Points represent hypothetical samples from different depths from the same package of sediment. The points will define a line, the slope of which is the $^{26}Al/^{10}Be$ ratio for the package of sediment. This ratio can then be used to calculate a burial age. The thick dark lines and points represent the change in slope that occurs with increased burial time for hypothetical data. As time after burial progresses the slope of the line will become less steep as both isotopes decay. The thin solid line represents a surface with constant exposure. The thin dotted lines are isochrones. They are the calculated ratio of $^{26}Al$ and $^{10}Be$ in the constant exposure surface after a set burial time. Figure from Balco & Rovey, 2008.

The concept of the isochron plot is shown in Figure 4. By plotting the $^{26}Al$ concentrations against $^{10}Be$ concentrations of several samples from different depths in the same layer, it is possible to define a line. The slope of this line is the $^{26}Al/^{10}Be$ ratio and can be used to calculate a burial age.

The line defined by the samples can then be compared to isochron lines corresponding to a simple burial history. These isochron lines are calculated based on the assumption that initial ratio of $^{26}Al/^{10}Be$ in the sample was 6.75 prior to burial. This would be the case if almost all of the TCN concentrations were produced in the depth profile. If the line defined by the measured data points fits onto or is parallel to the isochron lines, then the initial ratio for the samples was 6.75. If the slope of the measured points crosses the simple burial isochron lines, then the assumption is incorrect meaning that the sediment has experienced a complex burial history. The biggest weakness of the depth profile isochron method is that it can only be applied in situations where a paleosurface was exposed for a long period of time. The long exposure is what allows the gradient in $^{26}Al$ and $^{10}Be$

concentrations with depth to develop. If the period of exposure is not long enough, no gradient will develop and the method cannot be applied (Rybcynski et al., 2013).

The isochron method has also been done by collecting several cobbles from the same layer in a sediment deposit, instead of using a depth profile (Balco et al., 2013). The idea is that these large clasts probably originated from different parts of the catchment area before being buried together. This means each clast has come from a different location and has a slightly different history. This results in variations in the production rates of TCNs and erosion rates experienced by the clasts, which ultimately results in each individual clast having a different concentration of $^{26}Al$ and $^{10}Be$ (Balco et al., 2013). However, since all of the clasts came from the same catchment (should have the same initial $^{26}Al/^{10}Be$ ratio), and were all buried for the same amount of time (all experienced the same amount of decay), then they should have the same $^{26}Al/^{10}Be$ ratio. Since the cobbles should have the same ratio and should have various $^{26}Al$ and $^{10}Be$ concentrations, they can be used to define an isochron, from which a burial age can be calculated (as previously explained). The biggest weakness of this method, given that a sufficient number of cobbles are present at the sample site, is that the initial ratio of the cobbles must be assumed to be 6.75, and one must hope that the cobbles chosen during sampling have enough variation in TCN concentration to define an isochron.

*Grain size isochron method.*

In regions of high relief, which are frequented by landslides, it may be possible to avoid having to find a paleosol in order to apply the depth profile isochron method. In several cases in regions of high relief, where landslides are common, a variation in the concentration of TCNs with grain size has been observed (Brown et al., 1996; Belmont et al., 2007; Antinao, 2008; Puchol et al., 2014). For example, in the Cordillera Principal of the southern Central Andes, Antinao (2008) observed in sediments of major streams that $^{36}Cl$ concentrations were greater in the finer grain size fractions (Fig. 5). His grain sizes ranged from >0.25 mm to 4 mm.

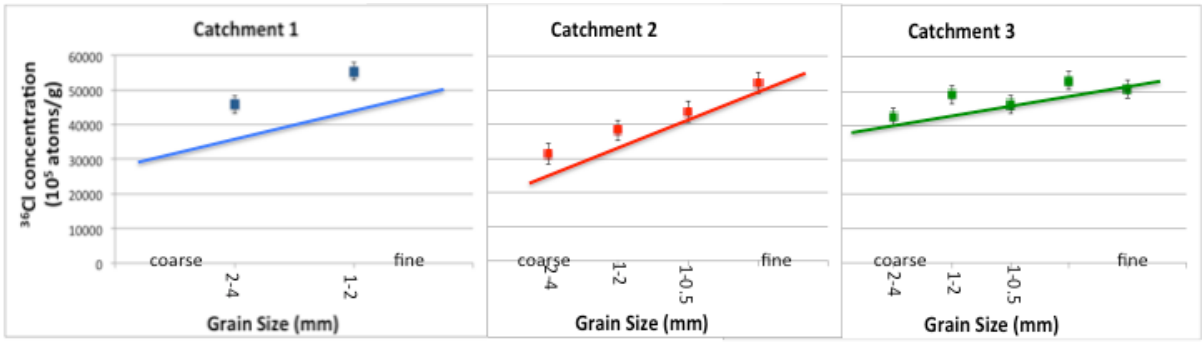


**Figure 5**: $^{36}Cl$ variation with grain size, in various catchments in the southern central Andes. Data from Antinao (2008)

Antinao (2008) concluded, along with Brown et al. (1995) who observed a similar relationship in streams in high relief areas of Puerto Rico, that the concentration dependence on grain size was linked to landsliding.

Consider the situation where an old mountain is being slowly and steadily eroded. In a low relief catchment, where much of the sediment is delivered to a stream by low-energy slope wash and diffusion processes, the majority of the sediments are fine, monomineralogic grains from the uppermost weathered portion

of regolith. On the other hand, in an active orogen, where slopes are steeper than 26°, a large portion of the sediment may be delivered by mass wasting processes (Antinao, 2008). The sediment delivered to the stream by mass wasting will comprise both the finer weathered material from the top of the weathered regolith, but also some larger, less weathered, multi-mineralogic fragments that are less easily comminuted in the short transport time. The finer grain sizes, being closer to the surface, experienced a higher cosmic ray flux resulting in more $^{26}Al$ and $^{10}Be$ production, whereas the coarser stream sediments were deeper and more shielded from cosmic rays, hence the grain size dependency. On average the sediment is derived from a few meters of regolith, which like the depth profile method, provides enough spread in the concentrations between the fine and coarse fractions to define an isochron (cf. Fig. 4 and Fig. 5), but the $^{26}Al/^{10}Be$ ratio through it should be approximately constant at 6.75. Using this method it should be possible to construct an isochron plot, but instead of using a depth profile that formed in a buried paleosol, this approach uses different grain sizes from a depth profile that formed in a mass-wasted regolith.


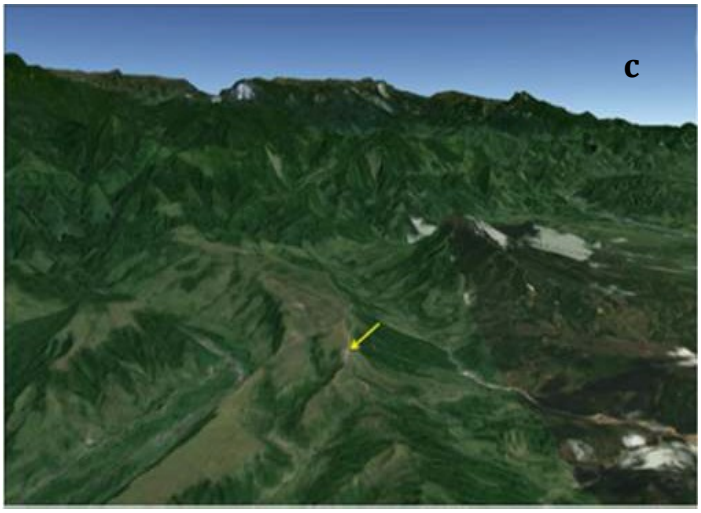


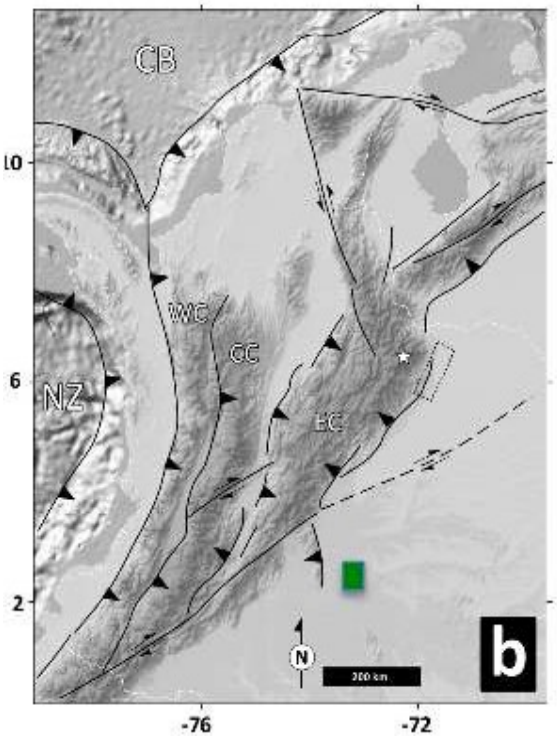


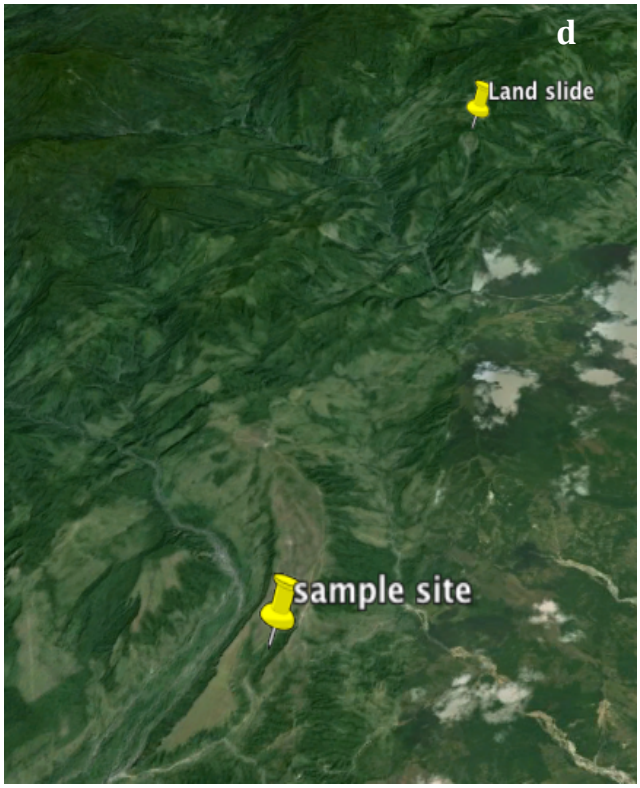


**Figure 6**: **A**. Map of South America, showing where the sample site (blue rectangle) is located.
Figure modified from Veloza et al, (unpub).
**B.** Regional map of the Colombian Andes. CB is the Caribbean Plate, NZ is the Nazca Plate and SA is the South American Plate. WC is the Western Cordillera, CC is the Central Cordillera and EC is the Eastern Cordillera. The green rectangle represents the sample site. Figure modified from Veloza et al, (unpub).
**C.** Over view of the sediment deposit for this thesis. The yellow arrow shows the sample site. Image from Google Earth.
**D.** Image showing proximity of the sample site to the mountain front and landslides. Image from Google Earth.
**E.** (Below) Sediment of the Guayabo Fm at the sample site. Photo from Mike Taylor.
**F.** (Below) Samples were taken from the base of this cliff face. The cliff has a height of 112m. Photo from Mike Taylor.


e


f

## 2.2 Geologic Setting

The study area for testing this new approach to isochron dating was chosen considering several factors: (i) access to sediments believed to be deeply buried for at least 1 Ma; (ii) the sediments were derived from a catchment with sufficiently steep slopes that landsliding is a significant mechanism for delivering sediment to streams; and (iii) the test results may also have an interesting geomorphological impact beyond technique development. The selected study area is located in the Tauramena locality of Colombia and is approximately 150 km NNE from Bogota.

The active tectonics of the region is currently being studied by M.Taylor at U. Kansas and his collaborators and research group. They required burial dating chronology to establish rates of fault slip. One of their sites close to a mountain front (with less opportunity of significant burial prior to final deposition) yielded a simple burial age of approximately 2.5 Ma (Veloza et al., Unpub), and they collected additional sample material to run this experiment.

The study area is located to the southeast of the triple junction between the Nazca, Caribbean and South American plates (Fig 6a). To the south the Nazca Plate is subducting under the South American Plate, forming a typical (little to no oblique components, clearly defined trench, established volcanic arc) convergent margin. However in the north, where interactions with the Caribbean Plate become important, an oblique component is added to the strain in the region (Cortez et al., 2006) Throughout the region are several thrust faults and strike-slip faults, which have accommodated uplift and deformation.

The Colombian Andes comprise three separate mountain chains, the Western Cordillera (Occidental), the Central Cordillera and Eastern Cordillera (Oriental) (Fig. 6b). The Western Cordillera is composed of layers of Cretaceous accreted sediment, separated by late Cenozoic aged thrust faults that verge roughly north-west (Cortes et al., 2006; Veloza, 2012). The Central Cordillera is an active volcanic arc, which was active since the Miocene. The Eastern Cordillera is a modern fold-and-thrust belt that formed from the structural inversion of a Cretaceous back-arc basin (Cortes et al., 2006; Gregory-Wodzicki, 2000). The inversion resulted in the conversion of normal faults to reverse faults and occurred in the Eocene (Cortes et al., 2006). This inversion was caused by a change in the stress regime from extension and transtension to a compressive regime that caused episodic uplift that continued to recent time (Cortes et al., 2006).

The study area is located on the eastern flank of the Eastern Cordillera (Fig. 6b,c,d). As previously stated, the region in which the sample site is located has been undergoing uplift since the Eocene. The sample site itself is a fluvial terrace composed of coble braided stream deposits (Fig. 6c). Due to its proximity to the mountain front it probably has a significant component of sediment derived from alluvial fans, however from the roundness and sorting of the sediment we can determine that the bulk of it is of fluvial origin. The sediment package is classified as part of the Upper Guayabo Formation, and is essentially a mixture of well-sorted, very coarse alluvial gravel and braided stream sediments (Parra et al., 2010) (Fig. 6e). The deposited gravel appears to exhibit horizontal bedding, imbrication, and good sorting (for a cobble gravel) which are consistent with their being fluvially

deposited, as opposed to deposition by debris flows or other gravity driven processes. Based on the range of clast roundness (Fig. 6e, from very rounded to subangular) some of the sediment has been transported in the stream for a long distance, but some of the sediment was deposited after a short transport distance. While it is possible that there may even be debris flows in this section, Taylor indicates that this was not observed but also that the sedimentology was not thoroughly examined.

The regional descriptions of the formation from literature describe it as a mix of channelized sandstones and conglomerates (braided channel deposits), horizontally stratified pebble to cobble conglomerates (alluvial fan deposits) and poorly stratified cobble to boulder conglomerates (debris flow deposits) (Parra et al, 2010). The sample site is in close proximity to shallow landslides that occur in the nearby mountains (Fig. 6d). These landslides are inferred to be a significant enough source of sediment that their TCN signature can be distinguished among all of the other processes that sourced sediment to the deposit.

A depth profile isochron burial age was attempted at the location in 2013 by Veloza et al, (unpub). Six samples were submitted for $^{26}Al/^{10}Be$ analyses at a US laboratory, however only four samples had a sufficient number of aluminum atoms to obtain $^{26}Al$ measurements, and the measurement precisions ranged from 57% to 143%. After blank subtraction, two of those samples yielded unacceptable results. The remaining two samples had 1-sigma $^{26}Al$ precisions of 57% and 70%, which was insufficient to obtain a depth profile isochron burial age. However, the simple burial ages (maxima) were calculated (Fig. 7) to be 2.65 ± 0.7 Ma and 2.25 ± 0.6 Ma. The

errors reported here and in Figure 7 only reflect the $^{10}$Be 1-sigma uncertainty to demonstrate what may be achievable with improved $^{26}$Al results, as the total error in the ratio was much greater than 100%, rendering the ages unacceptable.

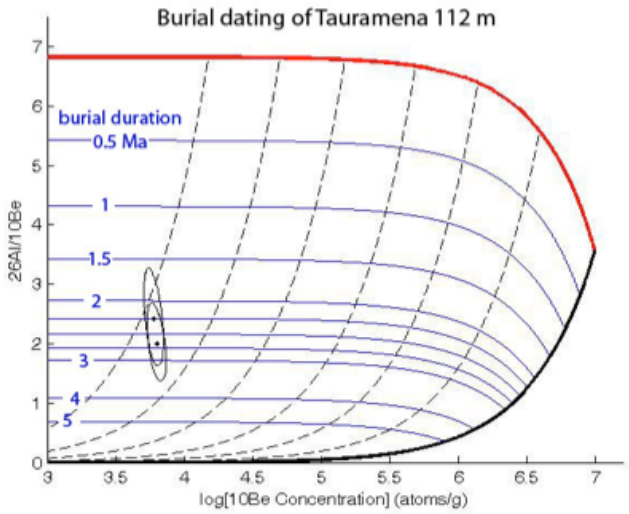


**Figure 7**: Simple burial plot of samples collected by Veloza et al. (unpub) from the sample site for this thesis.

In addition to the ideal location on the basis of the relief, age, and burial depth criteria, the preliminary age makes this a potentially very interesting sediment package considering landscape evolution at a major climate transition. These ages correspond approximately to the Pliocene-Pleistocene boundary at 2.6 Ma, which marks a significant change in global climate (Gibbard et al., 2010). The results of the thesis experiment may provide a better constraint on the age of the Upper Guayabo Formation and link climate change, not just tectonics, to mountain erosion and incision and increased sediment flux to the Andean foreland basin.

# 3.0 Methods

## 3.1 Field Methods

The field approach had the following objectives for testing the grain-size isochron burial dating method. Samples for any TCN burial dating method should be deep enough that they have been shielded from cosmic rays since their burial. For $^{26}Al/^{10}Be$, the mineral of choice is quartz, so the samples should have sufficient quartz (ultimately ca. 60 g of pure quartz in different grain sizes will be used). Site selection should also consider any natural or anthropogenic disturbance of the stratigraphy, and proximity to a paleosol.

The samples for this project were provided by Mike Taylor and Gabriel Veloza. As previously stated, the samples came from a fluvial terrace in the Colombian Andes. The site selected by Taylor and Veloza was ideal for burial dating because it exposed a steep (in places near-vertical) section of the formation with a height greater than 100 meters along a recently eroded riverbank (Fig 6f). The sediment was a mixture of several different grain sizes with a homogenous distribution. Samples in Veloza's original experiment were collected in five positions over a vertical distance of roughly 5 m, i.e. a depth profile.

The sediment received for this thesis experiment was a subsample of granules to fine sand from the five samples Taylor and Veloza collected. Those samples are from a very coarse gravel sequence in a fluvial terrace. The sample site is situated just a few kilometers beyond the modern mountain front (Fig 6b,c). The

samples were collected near the base of a deep gully that exposes over 112 m of the gravel above the modern stream (Fig 6f).

As previously mentioned, due to the wide range of grain size and roundness of the clasts it is likely that the sediment in the deposit originally was formed in a variety of processes before being transported and deposited by a fluvial system. Having sediment delivered to the mainstem stream from a wide range of surface processes will help produce a wider scatter in the TCN concentrations among different samples, and a wide concentration range is needed to more precisely define an isochron slope (if all of sediment had exactly the same concentration, i.e. each bag was a perfect mixture of a homogeneous population) then no isochron slope can be defined.

The biggest issue for collecting samples for burial dating is that the shielding of the samples must be taken into account. The amount of shielding will affect the amount of post-burial production of $^{26}Al$ and $^{10}Be$ (Gosse & Phillips, 2001). Post-burial production is due to spallation by neutrons and muons (Balco & Rovey, 2008). By blocking the flux of these cosmic rays, shielding decreases post-burial production. There are two major considerations when calculating the amount of shielding a site has. The first is the topography of the area, which takes into consideration how exposed the sample site is and whether any topographic features such as nearby mountains could block cosmic ray flux. The second consideration is the depth to which the sample is buried. All cosmic particles have an attenuation length, meaning that by increasing the depth of a sample, the flux of cosmic rays to the sample decreases (Gosse & Phillips, 2001).

For this particular project, shielding is not an issue for the samples since they were buried by more than 100 meters of sediment (Fig 6f). This thick sediment layer completely shielded the samples from cosmic rays meaning there would be negligible post-burial production. The only way that production may have occurred is by cosmic rays entering at shallow angles onto the steep face. However, because the cosmic ray flux is angular dependent (85% of the particles enter within a vertical 45° cone), the sample site was actually in a deeply and actively incising gulley cut into the river bank, and the sampled zones were cleaned (minimum 20 cm) before collecting the samples, post-burial production is considered very unlikely (Lal, 1991). Measurement of in situ cosmogenic $^{14}C$ in the samples would test this assumption.

The five ca. 3-kg samples with grain sizes ranging from pebbles to silt were collected with spades from six shallow pits in the section face 112.5 meters below the top of the sediment package and stored in triple-labeled double ziplock bags. While the depth profile method requires five samples collected in a vertical sequence, the samples for the grain size isochron method can be collected from a single thin layer, or, considering the precision of the technique will be greater than $10^4$ years, we could amalgamate samples over a 2 meter or thicker layer.

## 3.2 Lab methods

### 3.2.1 Physical Processing.

All processing for the grain size isochron burial dating method test was done using the facilities at the Dalhousie Geochronology Centre. Different grain size fractions were separated with a sieve shaker and 8" stainless steel sieves. Originally it was hoped that each sample would have its own set of TCN samples with distinct grain sizes. However there was a lack in quartz mass in certain grain sizes for particular samples, meaning that in order to be able to run the samples, the sediment remaining from all five pits had to be combined. The initial size fractions were >8, 8-4, 4-2, 2-1, 1-0.85, 0.85-0.5, 0.5-0.355, 0.355-0.250, 0.25-0.15 mm, but it was anticipated that two or more of these fractions may need to be combined in order to obtain 60 g of pure quartz for each grain size fraction.

Before chemical processing could begin the all of different grain size fractions had to be crushed to the same grain size, which would also optimize chemical dissolution. A fine grain size is not desirable because it increases the rate at which dissolution in hydrofluoric acid (HF) occurs, making it more likely that too much quartz will be undesirably dissolved. However the sample has to be fine enough that each grain is a single mineral phase. For this project the optimum grain size, considering that the limited lab time required aggressive use of HF, was 0.355-0.250mm. Grain sizes smaller than 0.355-0.250 mm were not physically processed. The coarser grain size fractions were put through a jaw crusher and all of the grain

size fractions were put through a disk mill in order to reduce them to the optimum grain size.

3.2.2 Chemical Processing.

After each grain size fraction was reduced to the selected grain size, mineral separation and quartz purification began. The goal of chemical processing is to the isolate the quartz fraction for each sample without losing much quartz. Typical quartz efficiencies are 40%, including a step that intentionally dissolves 35% of the quartz to remove any meteoric $^{10}$Be (Kohl & Nishiizumi, 1992). First the samples were boiled in aqua regia. This dissolved weaker minerals such as micas and removed many of the metals. Next the samples were briefly exposed to hydrofluoric acid to weaken the silicate phases in the samples.

The bulk of the dissolution of non-quartz phases was done in the next step where the samples were split up into small bottles that were then filled with hexafluorosilicic acid (F6 acid). Because of its ability to break Al-O bonds but not Si-O bonds, this acid dissolves non-quartz silicates, and leaves quartz relatively unaffected (Rees-Jones, 1995). This was the first time that F6 acid was used in a systematic way in the DGC cosmogenic lab, and therefore as part of this thesis research a series of tests was designed to optimize the efficiency of the dissolution. The F6 optimization tests involved varying the mass of sample between 10-30 g and the volume of acid, pretreating the samples with concentrated HF, and heating the bottles at different temperatures. A hot dog roller was purchased to constantly mix the samples and keep them at an optimum temperature. The optimum procedure was to place 20 g of sediment, boiled in concentrated (46%) HF for 20 minutes, into

a 250 ml HDPE bottle with 50 ml of F6, on the hot dog roller with temperature setting approximately 60°C. Care needed to be taken to ensure the caps were securely fastened, that the bottles were each vigorously shaken by hand at least once each day, and that pressure was released daily by briefly loosening the cap. This F6 procedure lasted for weeks for each sample and because such large masses of pure quartz were needed to ensure sufficient $^{10}$Be and $^{26}$Al precision, many samples had to be split into different containers to speed dissolution.

Following this the samples were exposed to dilute hydrofluoric acid and placed in ultrasonic tanks for aggressive dissolution of the quartz. The ultrasonic tanks heated the samples to 95°C and sped up the dissolution process significantly. The goal of this step was to dissolve the outer part of the quartz grains, to ensure the removal of any meteoric $^{10}$Be as well as to dissolve any remaining non-quartz minerals (Kohl and Nishiizumi, 1992). This was done over several days until the mass of the sample decreased by one third. To test for quartz purity, a combination of reflected light microscopy and ICP-OES (Inductively Coupled Plasma-Optical Emission Spectrophotometer) analysis for aluminum was used.

While all quartz has some aluminum (10 to 90 ppm), most of the aluminum would come from other minerals. It was important keep the aluminum as low as possible (quartz as pure as possible) in order to minimize the amount of native aluminum, which makes the ion chromatography difficult (see below), and to maximize the $^{26}$Al/$^{27}$Al measured by AMS (Accelerator Mass Spectrometer). The previous attempts at this site obtained very low ratios (10-15) that contributed to the high measurement error.

### 3.2.3 Element extraction

Element extraction. Next was the extraction and isolation of aluminum and beryllium. For this part of the process it was decided 60 g of sample was needed. This much mass was not present for the upper four grain sizes (>8, 8-4, 4-2, 2-1 mm) so they had to be combined into a single sample.

First, I rinsed the samples with double-deionized boron-free Type 1+ (18.2 MOhm water). Once the samples were dried, I precisely weighed (0.1 milligram precision) them before they were completely dissolved in 50-100 mL of ultrapure hydrofluoric acid with nitric acid (to prevent the formation of insoluble $CaF_2$). Next G. Yang (DGC) used three to five milliliter of ultrapure perchloric acid to remove the remaining HF by evaporation (perchloric acid has a higher boiling point). Eventually the precipitates were dried, re-dissolved, and dried again to ensure most of the HF had been removed. At the end of the process the samples were dissolved in nitric acid. At this point the samples were brought up to 100 mL in ultrapure 2% $HNO_3$, and a 5 mL aliquot of each sample was collected, gravimetrically, for high precision analysis for Be, Al, and Ti on the ICP-OES. The remaining 95 mL was evaporated to near-dryness, dissolved in HCl, centrifuged in 10 mL test tubes, and the supernate decanted in preparation for ion chromatography.

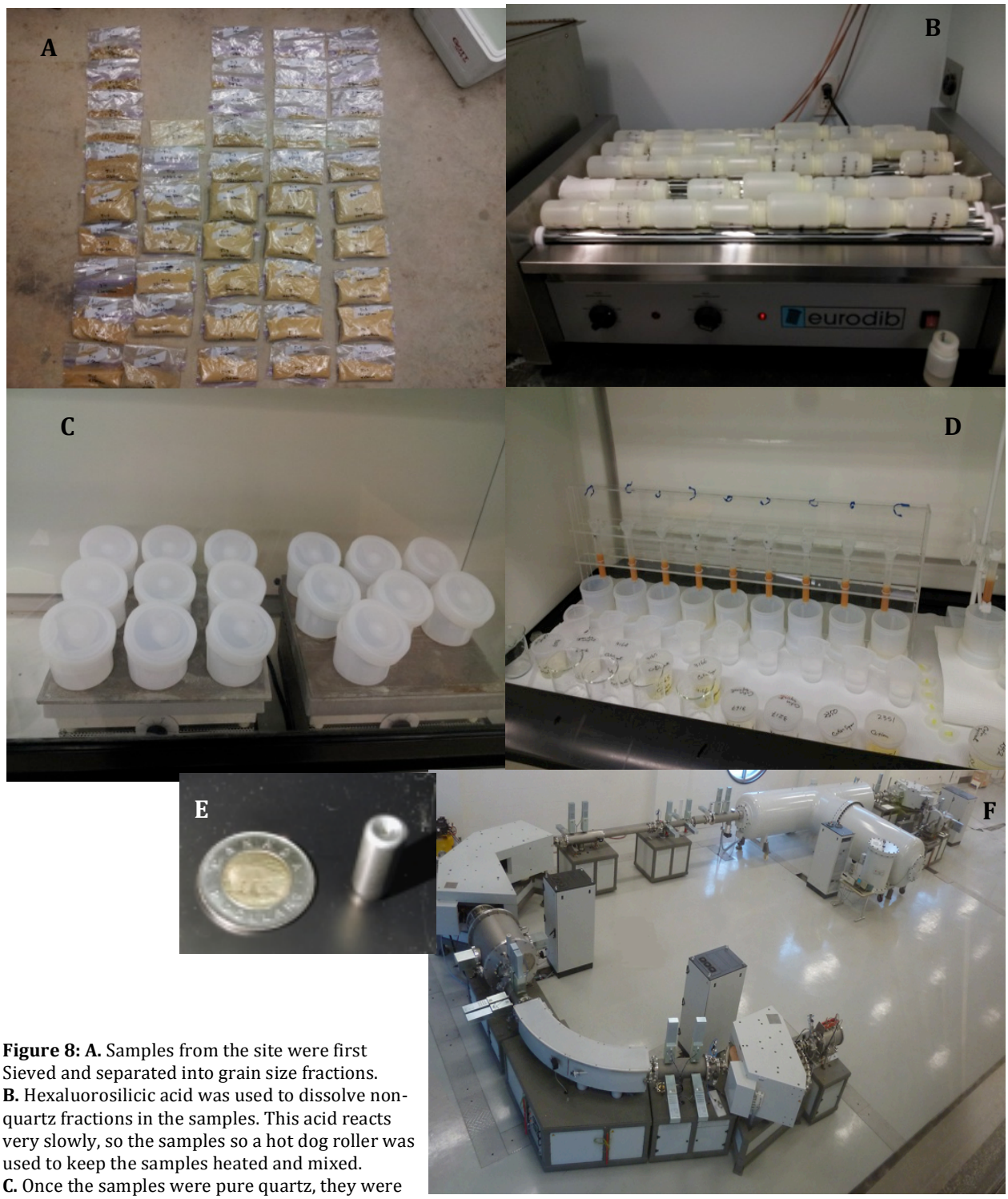


**Figure 8: A.** Samples from the site were first Sieved and separated into grain size fractions.
**B.** Hexaluorosilicic acid was used to dissolve non-quartz fractions in the samples. This acid reacts very slowly, so the samples so a hot dog roller was used to keep the samples heated and mixed.
**C.** Once the samples were pure quartz, they were fully dissolved in hydrofluoric acid.
**D.** Column chemistry was used to extract the aluminum and beryllium out of the samples.
**E.** Once aluminum and beryllium were extracted as oxides, they were packed into steel targets before being sent to the AMS.
**F.** A photo of an AMS (Accelerator Mass Spectrometer) at the university of Ottawa. The AMS used to analyze samples for this thesis is at Lawrence Livermore National Lab.
Photos **A, B, C, D** from Sean Des Roches. Photos **E, F** from John Gosse.

Next G. Yang ran the samples through anion and cation columns to isolate the aluminum and beryllium. These columns were filled with resins that exchange anions and cations by varying the normality and volume of HCl eluent. By using these columns aluminum and beryllium was extracted from the sample as $AlCl_3$ and $BeCl_2$. The large aluminum concentration and large sample mass required that we ran the samples through the columns twice. Once these elements were extracted they were converted into hydroxides with ultrapure ammonia gas, and ignited to form oxides of the two metals. The oxides were then mixed with ultrapure niobium metal powder, and packed into clean stainless steel target holders by G. Yang.

There were several deviations from the normal chemistry procedure used at DGC. Since the concentrations of TCNs in the quartz were anticipated to be low, from the work by Veloza et al, (unpub.), certain alterations to the chemistry procedure had to be made. Less carrier was added to the samples to make sure that the $^{10}Be/^{9}Be$ ratio of the process blank (receives no quartz, only the $^{9}Be$ carrier), is significantly smaller than the ratio measured in the samples. A typical ratio of $^{10}Be/^{9}Be$ for a process blank is $1.5 \times 10^{-15}$ ( for $^{27}Al/^{26}Al$ it is $2 \times 10^{-15}$). Having less carrier in the samples means there are less atoms present, which may decrease the Be current during AMS and result in less accurate measurements.

Due to the low TCN concentrations of the samples, greater than usual amount of quartz had to be used. Typically 20-25 g of quartz is dissolved, however for this experiment 60 g of quartz was needed to ensure a radioisotope abundance above background. Using more mass can increase the amount of unwanted cations that need to be separated out of the samples. The aluminum and beryllium are separated

from other cations during column chemistry. If there are too many cations in the sample they overwhelm the columns, making them less effective at retaining of aluminum and beryllium, which can result in the loss of those target elements.

A third departure from normal chemistry procedure was needed to compensate for the high mass of quartz and therefore high abundance of unwanted cations. Before column chemistry a pH-controlled precipitation of the aluminum and beryllium was done by converting them into $Al(OH)_3$ and $Be(OH)_2$ precipitates, centrifugation, and decanting the supernates containing the unwanted cations. During this step the beryllium and aluminum hydroxides may have been partially redissolved (their solubility has a wide pH range) and aluminum and beryllium could have been lost to the supernate.

### 3.2.4 AMS measurement

To measure the concentrations of $^{26}Al$ and $^{10}Be$, the oxide targets were sent to Lawrence Livermore National Lab to be analyzed by an AMS. The AMS did not actually measure the absolute amounts of $^{26}Al$ and $^{10}Be$. Rather it measured the ratio of $^{26}Al/^{27}Al$ and $^{10}Be/^{9}Be$ (Gosse & Phillips, 2001). $^{9}Be$ does occur naturally, but in concentrations too low to influence the analysis, so before the quartz was dissolved approximately 210 mg of $^{9}Be$ was added as a carrier to the beryllium sample. The carrier was produced at the DGC using a phenacite crystal collected from a deep Ural Mountain mine, and has negligible $^{10}Be$. The mass of carrier added was precisely recorded. For the aluminum sample, $^{27}Al$ is naturally abundant in the quartz, so no carrier was necessary (Gosse & Phillips, 2001). Instead the

concentrations of aluminum were measured on an ICP-OES. $^{27}Al$ is twelve or more orders of magnitude more abundant than the cosmogenic $^{26}Al$, so the aluminum concentration measured by the ICP-OES can be assumed to be the concentration of $^{27}Al$ (Gosse & Phillips, 2001).

Since the ratios of $^{26}Al/^{27}Al$ and $^{10}Be/^{9}Be$ were measured by the AMS and the concentration of $^{27}Al$ (measured by ICP-OES) and $^{9}Be$ (known amount of carrier was added to each sample and also verified with ICP-OES) were known, it was possible to calculate the concentrations of $^{26}Al$ and $^{10}Be$ for the samples.

## 3.3 Computation

The production of TCN is mainly due to spallogenic interactions of sediment with fast neutrons, negative muons and fast muons (Lal, 1991). The concentrations of TCN in sediment depend on several factors. The concentration of a general cosmogenic nuclide in sediment can described by the equation:

Eq.1 $$N_m = \frac{P(0)}{\lambda + {\varepsilon}/{\Lambda}}\, e^{-\lambda t} + \frac{P(z)}{\lambda}\left[1 - e^{-\lambda t}\right]$$

where $N_m$ is the measured concentration for the nuclide (atoms $g^{-1}$), P(0) is the production rate of this nuclide at surface (atoms $g^{-1}$ $yr^{-1}$), P(z) is the production rate of the nuclide at a particular depth (atoms $g^{-1}$ $yr^{-1}$), $\lambda$ is the decay constant of the nuclide, $\varepsilon$ is the erosion rate for the surface (g $cm^{-2}$ $yr^{-1}$), $t$ is the burial time (yr) and $\Lambda$ is the attenuation length of a particular particle (g $cm^{-2}$) (Balco & Rovey, 2008).

For each TCN, three calculations must be done, one for each type of cosmic ray that produces nuclides, because each type of particle has different attenuation

lengths and production rates (Gosse & Phillips, 2001). There are two terms summed in Equation 1. The first term represents the inherited concentration of the sample, which is the amount of a nuclide in a sample before deposition. The second part of the equation represents the amount of post-depositional production in the sediment, i.e. the production that would generate measurable TCN concentrations in a depth profile if the surface was exposed for a sufficient time (Balco & Rovey, 2008).

Before sediment is buried, it is exposed in a catchment area for a time where its inheritance of $^{10}$Be and $^{26}$Al develops (Gosse & Phillips, 2001). The build up of these cosmogenic nuclides in sediments can be described by a simplified version of equation 1:

Eq.2 $$N_m = \frac{P(0)}{\lambda'} e^{-\lambda' t_i}$$

with Eq.3 $$\lambda' = \lambda + \frac{\varepsilon * \rho_r}{\Lambda_i}$$

with $\lambda'$ as the effective attenuation length taking into consideration the erosion or aggradation rate, $\rho_r$ as the density of the sediment (g cm$^{-3}$) and $t_i$ as the exposure time of the surface (yr).

Since the properties of the sediment (e.g. bulk density), the cosmic rays (e.g. flux, production rates) and the nuclides (e.g. decay rates) are considered constant over time, we can see from Equation 2 that the concentration and ratio of the nuclides are controlled mostly by the erosion rate in the catchment and the exposure time once the sediment is deposited (Balco & Rovey, 2008) (Fig. 9).

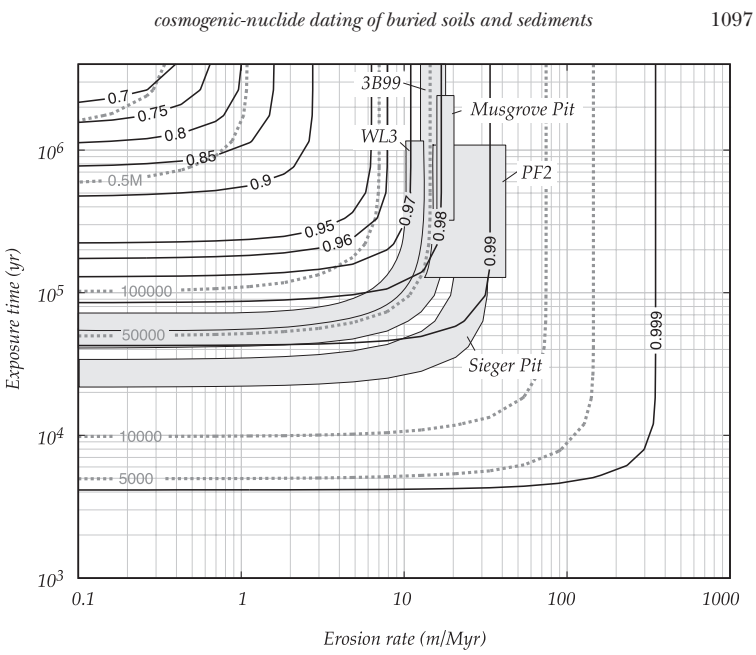


**Figure 9**: Plot showing how the ratio of $^{26}Al/^{10}Be$ deviates in sediments from the production ratio (6.75) with various exposure times and erosion rates. Having high exposure time and low erosion rates results in the largest deviance due to saturation of the nuclides being reached in the soil (Balco & Rovet, 2008)

Figure 9 shows that variation of the ratio of $^{26}Al/^{10}Be$ from the production ratio (6.75) due to changes in the erosion rate and exposure time (Balco & Rovey, 2008). The graph shows that samples with high erosion rate and low exposure time have $^{26}Al/^{10}Be$ ratios that are closer to the production ratio since they do not have enough time to become saturated in $^{26}Al$ and $^{10}Be$ (Balco & Rovey, 2008).

With this in mind, let us consider the samples collected for this thesis. The samples began as regolith along slopes in a catchment with high relief that was prone to landslides (we can ignore the previous histories of the samples because they are irrelevant if longer than about eight half lives of $^{10}Be$). Though there were frequent landslides, the surface was still experiencing steady erosion over time. This erosion kept the surface from saturating in cosmogenic nuclides, meaning that that the ratio of $^{26}Al/^{10}Be$ should have been close to 6.75 (Balco & Rovey, 2008). The surface processes and landslides would deliver grains of various sizes and concentrations of $^{10}Be$ and $^{26}Al$ and, with the exception of rare deep-seated

landslides that deliver bedrock fragments that have higher $^{26}Al/^{10}Be$ due to muonic production (e.g. 8.2), the ratio of the average inherited $^{26}Al/^{10}Be$ in the sediment will be 6.75, assuming no prolonged burial during storage (i.e. for more than a hundred thousand years) (Balco & Rovey, 2008).

No definitive paleosol was recognized at the sample site, so considering the tropical climate, the samples were most likely buried reasonably quickly (i.e. no sample was exposed for more than about 10 ka before being buried). This means that almost all $^{26}Al$ and $^{10}Be$ measured in the samples can be attributed to inheritance. Of course this is not possible to demonstrate in the field, and will only be known after evaluating the TCN-grain-size relationship. If the samples were exposed for more than 10 ka, the TCN dependency with grain size would not be visible.

Using the assumption that all of the nuclides in the sediment formed before burial in the catchment, then their concentrations would have only decreased after burial due to radioactive decay. It is not possible for us to know what the absolute initial concentrations of $^{26}Al$ and $^{10}Be$ were in the samples unless we determine the age, and then correct for the loss of TCN due to decay (Balco & Rovey, 2008). The $^{26}Al/^{10}Be$ in a sample will change predictably according to the different radionuclide decay rates, and at any given time all of the samples for the different grain size would have the same ratio, assuming they all began at 6.75 (Balco & Rovey, 2008).

## 3.4 Error mitigation and analysis

During physical processing several precautions were taken to control error. Only one sample was ever processed at a time, and between samples all sieves, machinery and surfaces were thoroughly cleaned. All samples were stored in clean Ziploc bags that were labeled several times.

During chemical processing all jars that held samples were labeled several times, and the jars were always kept covered whenever possible. The lab doors were kept closed, and the lab has a dedicated boron-free HEPA-filtered HVAC air purification system. Only ultrapure reagents and water were used after the initial stages of quartz purification. All masses were determined with high-precision balances. With the exception of the Teflonware and target holders, all containers were virgin materials. The precision of the ICP-OES measurements for beryllium and aluminum were typically better than 2%, so considering this and gravimetric uncertainly of much less than 1%, the total internal random error contributed by the chemistry is considered 2% at 1-sigma. AMS error is based on the Poisson distribution-based precision, and is therefore dependent on the number of counts of atoms. Error contributed by the blank subtraction is typically negligible because the process blanks have low ratios ($1.5 \times 10^{-15}$), however if the samples were buried for millions of years, the ratios in the samples may be comparable, and the uncertainty in the blank subtraction can be the dominant source of measurement error.

For the calculations several assumptions were made. The assumption was made that the erosion rate in the catchment was simple, meaning that it was

constant over time, with occasional landslides. The assumption was made that during the transport of the samples from the catchment to the site of burial the samples were not stopped at any point and exposed at surface. As well the assumption was made that the burial of the samples was rapid and complete.

The AMS and ICP-MS measurements have systematic error that must be taken into account. Error calculations are shown in Appendix 1.

## 4.0 Results

Accelerator Mass Spectrometer (AMS) analysis of the samples was conducted at Lawrence Livermore National Lab. Two separate analyses were done, one for $^{26}Al/^{27}Al$ and one for $^{10}Be/^{9}Be$ (Appendix 1). The AMS and chemical data (e.g. carrier and quartz masses, blank subtractions, and native aluminum and beryllium in the quartz as measured by ICP-OES at DGC) were then reduced to calculate the concentrations of $^{26}Al$ and $^{10}Be$ in the quartz samples, in atoms per gram. $^{27}Al$ is naturally much more abundant than $^{26}Al$, so we can assume that the aluminum concentration measured by the ICP-OES represents the concentration of $^{27}Al$ in the sample. By multiplying the $^{27}Al$ concentration (in atoms per gram of quartz) by the $^{26}Al$ /$^{27}Al$ ratio measured by the AMS, the $^{26}Al$ concentration for the sample can be calculated.

For the beryllium samples, native $^{9}Be$ does not occur naturally in high enough concentrations in quartz (e.g. beryl inclusions) to help carry the $^{10}Be$ through the chemistry (0.1 μg/g or less beryllium). Therefore a beryllium carrier (averaging 211 μg of $^{9}Be$) was added to the quartz at the beginning of chemistry. Since the amount of carrier added was precisely measured we can calculate the amount of $^{9}Be$ in the sample. So, the $^{10}Be$ concentration is determined by multiplying the $^{9}Be$ atoms from the carrier by the $^{10}Be$ /$^{9}Be$. The full data reduction process is shown in a spreadsheet, in Appendix 1. The data are shown in Table 1 below.

| Sample name | $^{10}$Be Conc | $^{10}$Be Unc | $^{26}$Al Conc | $^{26}$Al Unc | $^{26}$Al/ $^{10}$Be Ratio | Ratio Unc |
|---|---|---|---|---|---|---|
| comb3159-3162 | 4078 | 312 | 41902 | 9218 | 10.3 | 2.40 |
| TAME0.85-1 | 4676 | 321 | 31565 | 6944 | 6.8 | 1.56 |
| TAME0.5-0.85 | 8137 | 922 | 27869 | 6131 | 3.4 | 0.84 |
| TAME0.335-0.5 | 6654 | 309 | 31897 | 7017 | 4.8 | 1.07 |
| TAME0.25-0.355 | 6437 | 272 | 36785 | 8093 | 5.7 | 1.28 |
| TAME0.150-025 | 5909 | 311 | 41867 | 9211 | 7.1 | 1.60 |

**Table 1**: Concentrations of $^{26}$Al and $^{10}$Be for the samples taken for this thesis are in the table above. Values are the result of the data reduction of the AMS data. All concentrations are in atoms/g

The reason why the TAME 0.5-0.85 beryllium data is colored red is because there was only enough BeO in the target for the AMS to do a single beryllium measurement. After the first run, the current was too low to proceed. This means that the data for this sample is unreliable, so it will not be used in further analysis. Reasons for this are listed in the Discussion section.

The uncertainties for the $^{10}$Be and $^{26}$Al measurements (4-8% and 22% at 1-sigma), which include uncertainties in the process blank subtraction and chemistry error (2%, mostly from ICP measurement) are higher than normal (e.g. for the measurement of the isotopes in 20 g quartz from a boulder). This is partly because of the very low abundance of $^{10}$Be (i.e. 6000 atoms/g is much lower than the typical $10^5$ atoms/g) but also because of challenges in chemistry when running so much quartz with less than the normal amount of beryllium carrier (250 μg). Likewise, the samples had high aluminum concentrations, which with such large masses of quartz, caused changes to the elution of the aluminum and beryllium cations during ion chromatography.

# 5.0 Discussion

## 5.1 Interpretations of TCN data

### 5.1.1 Hypothesis 1- Grain-size dependent isochron method is viable

The concentrations of $^{26}Al$ and $^{10}Be$ were plotted onto an isochron plot in an attempt to determine a burial age. The isochron plot is shown in Figure 10 below.

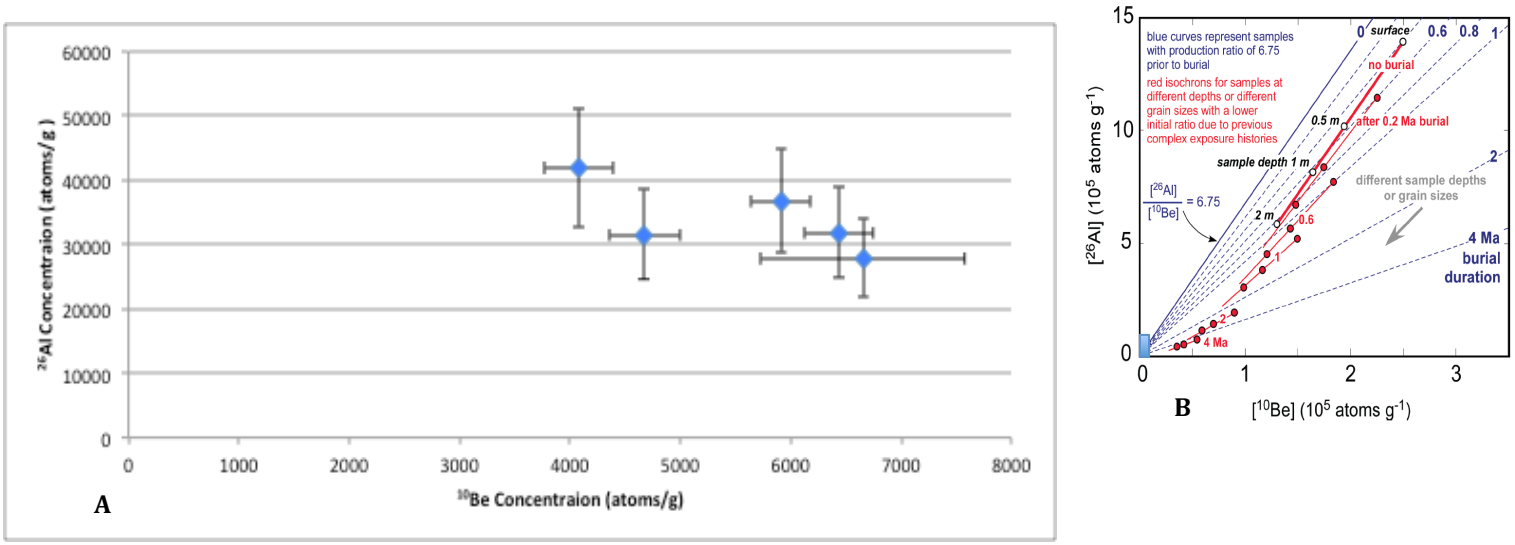


**Figure 10**: **A.** Isochron plot of samples from the Tauramena sample site.
**B.** What is considered a typical isochron. The blue box represents where the data from this thesis would plot. Figure adapted from Balco & Rovey 2008.

From the isochron plot we can see that the data defines a negative slope. This is not an acceptable outcome on the isochron burial plot (has a positive slope) so the data cannot be used to calculate a burial age. Thus the data suggest that the hypothesis that an isochron chronology can be achieved using grain-size fractions is false.

The most likely reason that these data did not work out was due to very low concentrations of the elements being present in the AMS targets. The number of atoms stripped from the oxide target and forming a beam of $^{27}Al$ or $^{9}Be$ during AMS is recorded as a current. The currents for both our aluminum and beryllium measurements were a factor of 5X smaller than normal (Appendix 1). A low current usually indicates that there is a problem with the chemical preparation of the target, because there is insufficient aluminum or beryllium in the target, or there is some other atoms in the target that are interfering with the aluminum and beryllium atoms when they are sputtered. In this instance, it is likely that the chemistry purified the targets sufficiently. In fact, for these targets, two additional steps were taken to do this. First, between the anion column chemistry and cation column chemistry, the samples were precipitated in a buffered solution to separate alkali and alkaline earth elements from the beryllium and aluminum. Second, an additional cation column chemistry was conducted to better separate aluminum and beryllium from other impurities. Because of the large mass and therefore potentially high abundances of these other unwanted cations, it is believed that a significant mass of aluminum and beryllium were both lost during the chemistry procedures. Additionally, because aluminum was very high, there was aluminum in the BeO target, which may have contributed to a lower current. Furthermore, because 16% less beryllium carrier was added to help keep the ratio of $^{10}Be/^{9}Be$ in the samples high relative to the process blank, this contributed to a lower current.

In addition to the low current, a low abundance of the radioisotopes $^{10}Be$ and $^{26}Al$ was anticipated (hence the lower carrier mass added). The low abundance is

caused by a long burial period during which the radioisotopes decay. This lower abundance has resulted in an insufficient number of atoms being detected to obtain a higher precision. Precision is described by the Poisson distribution, which can be estimated as $\frac{1}{\sqrt{n}}$ where *n* is the number of atoms of the radionuclide measured. To obtain a 1% precision, 10,000 counts need to be detected, whereas the $^{26}Al$ samples yielded 11 counts or less per 400 second run (three runs were attempted) and $^{10}Be$ had less than 150 counts total.

There may be other factors that influenced the poor performance of the oxides. During the dissolution of quartz with HF, the fluorine in the acid can react with calcium to form $CaF_2$ crystals, which can scavenge aluminum and beryllium as inclusions. Steps are taken to avoid these processes (e.g. the addition of a small amount of nitric acid) but they can still occur on the small scale and result in the loss of Al, at a rate that would be different for each sample, depending on the abundance of unwanted cations. This is unlikely as no crystals were observed after dissolution.

Another possibility is that some of the quartz crystals dissolved had an inclusion on beryl. This would be a large source of $^{9}Be$ and would cause low measurements of the $^{10}Be/^{9}Be$ ratio on the AMS. This does not appear to be the case, because measurements of beryllium in quartz before dissolution did not indicate anomalous beryllium concentrations, and because the $^{10}Be$ concentrations are similar to the concentrations achieved previously by PRIME Lab.

Therefore, while the results suggest that H1 is false, it is possible that with samples from a region with lower erosion rates, or a different chemistry procedure and better current but at lower precision, a positive result could be achieved.

5.1.2 Hypothesis 2- High erosion rates in landslide prone regions will cause imprecision

As previously stated, one of the reasons that the AMS measurements were such low concentrations can probably be attributed to a low initial TCN concentration in the samples, which is a result of rapid erosion rates in the catchment area of where the samples originated. It appears that the hypothesis that high erosion rates in the catchment area of the sediment would decrease TCN concentrations below a point where they could not be resolved holds true.

The paleo-erosion rates of the catchment area can be calculated with the collected $^{10}$Be and $^{26}$Al data individually following the method presented by Schaller et al. (2002) and Hidy et al. (2010). Essentially this involves correcting the measured radioisotope concentration for loss by decay during the burial time. While the burial duration is uncertain in this case, estimates from two measurements from Veloza et al. (unpub.) were 2.25 and 2.65 Ma. Therefore, assuming a 2.5 Ma burial duration, the measured concentrations, corrected for decay, are interpreted as the concentrations of the TCN in the sample at the time of deposition. This then can be used to calculate erosion rate with the equation:

Eq.4 $$\varepsilon = \frac{C^{\circ}\Lambda}{P^{\circ}\rho}$$

where $\varepsilon$ is the erosion rate (cm yr$^{-1}$), $C^{\circ}$ is the TCN concentration at the time of deposition (atoms g$^{-1}$), $\Lambda$ is the attenuation length of a cosmic ray (g cm$^{-2}$), $P^{\circ}$ is the production rate for a particular TCN in a catchment area (atoms g$^{-1}$ yr$^{-1}$) and $\rho$ is the bulk density of the material (g cm$^{-3}$). Full calculations are shown in Appendix 1.

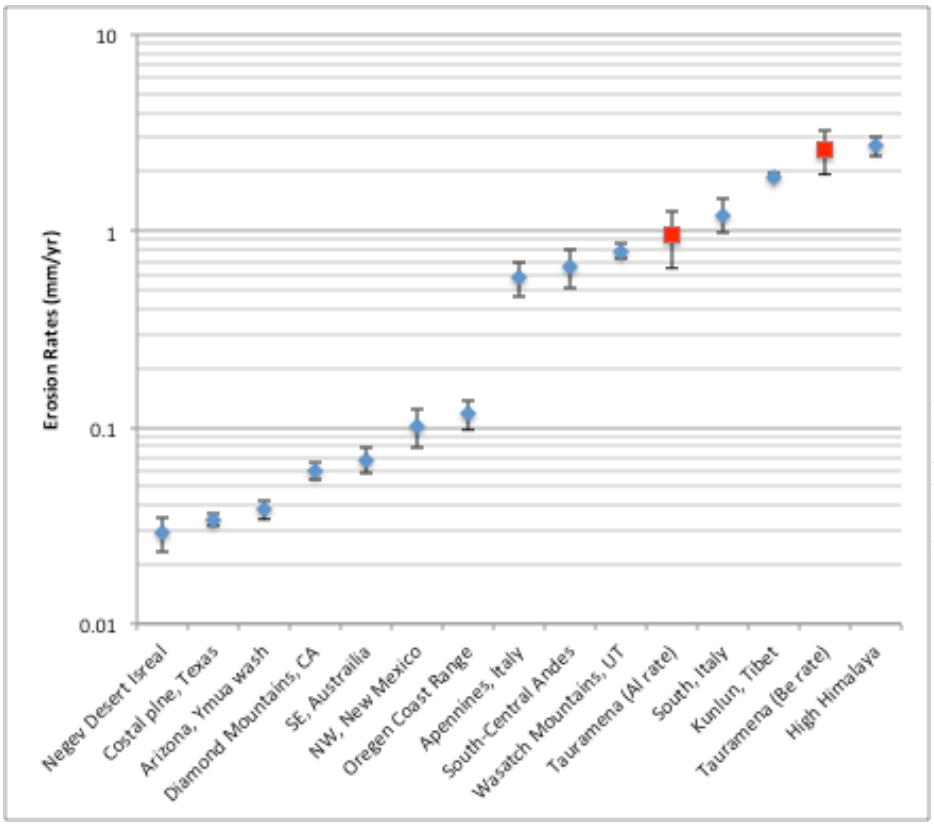


**Figure 11**: Paleo-erosion rates calculated from the $^{26}Al$ and $^{10}Be$ data. A sample of modern catchment-wide erosion rates have also been plotted for comparison. The red squares are the measured erosion rates. The blue diamonds are erosion rates from literature. See Table 2 for a list of references.

| | |
|---|---|
| Negev Desert Isreal | Clapp et al., 2000 |
| Costal plne, Texas | Hidy et al., 2014 |
| Arizona, Ymua wash | Clapp, Bierman & Caffee, 2002 |
| Diamond Mountains, CA | Granger et al., 2001 |
| SE, Austrailia | Heimsath et al., 2000 |
| NW, New Mexico | Clapp et al., 2001 |
| Oregen Coast Range | Heimsath et al., 2001 |
| Apennines, Italy | Cyr & Granger, 2008 |
| South-Central Andes | Atinao, 2008 |
| Wasatch Mountains, UT | Stock et al., 2009 |
| South, Italy | Cyr et al., 2010 |
| Kunlun, Tibet | Dingd et al., 2003 |
| High Himalaya | Vance et L., 2003 |

**Table 2:** References associated with localities and erosion rates plotted in Figure 11.

The erosion rates calculated using the aluminum and beryllium data from this thesis are shown in Figure 11 as red squares. A sampling of erosion rates from around the world has also been included to provide comparison. It is apparent in the diagram that there is a significant difference in the calculated erosion rates given by the different isotopes. $^{10}Be$ gave an erosion rate of 2.59±0.65 mm $yr^{-1}$ and $^{26}Al$

gave an erosion rate of 0.96±32 mm $yr^{-1}$. This discrepancy was caused by having too much $^{26}Al$ in the sample (likewise we could say there was too little $^{10}Be$).

The extra $^{26}Al$ could be the result of several factors. First this could be caused by errors in the chemistry, most likely during the sample purification. The high $^{26}Al$ could also been a result of an incorrect assumption of the initial $^{26}Al/^{10}Be$ ratio. We assume the ratio is 6.75, but if the sample has undergone a complex burial history, this may not be true. As well, if the assumption made about the burial age of the sediment is incorrect too much $^{26}Al$ may have been calculated to be present in the sample at the time of deposition. Since $^{26}Al$ has a faster decay rate than $^{10}Be$, a correction for an age which is too old will result in too much $^{26}Al$ being calculated for the sample prior to deposition.

Going back to Figure 11, the paleo-erosion rates obtained from the $^{10}Be$ and $^{26}Al$ are consistent with modern erosion rates determined for wet, high relief, tectonically-active orogens elsewhere in the world. The erosion rate from the $^{10}Be$ data compares with 2.7 mm $yr^{-1}$ at the High Himalayas and 1.9 mm $yr^{-1}$ at Kunlun, Tibet from modern samples. The erosion rate from the $^{26}Al$ data is bracketed by 1.21 mm $yr^{-1}$ in Southern Italy and 0.79 mm $yr^{-1}$ at the Wasatch Mountains, Utah.

Unfortunately, because the calculated paleo-erosion rates are over an uncertain burial duration, and their measurements are imprecise, and because the geometry of the catchment may have changed significantly so that the catchment-average production rate used may also be incorrect, they are only general estimates of the actual paleo-erosion at best.

5.1.3 Was there a grain size dependence?

The measured data do not provide a $^{26}Al$ vs. $^{10}Be$ isochron. A probable reason for this is related to difficulty in conducting chemistry on a large sample with such low TCN abundance, as discussed above. However, one of the critical assumptions of the method was that there is a grain-size dependency among the TCN concentrations, owing to decreases in concentration and weathering with depth in regolith on the catchment surface. To determine if the data reveal any indication of this grain size dependency, the relationship between $^{10}Be$ and $^{26}Al$ and grain size was investigated.

The $^{10}Be$ concentrations show no variation with grain size, likely because their low production rates did not provide sufficient scatter beyond the total analytical uncertainty after millions of years of decay (Fig. 12).

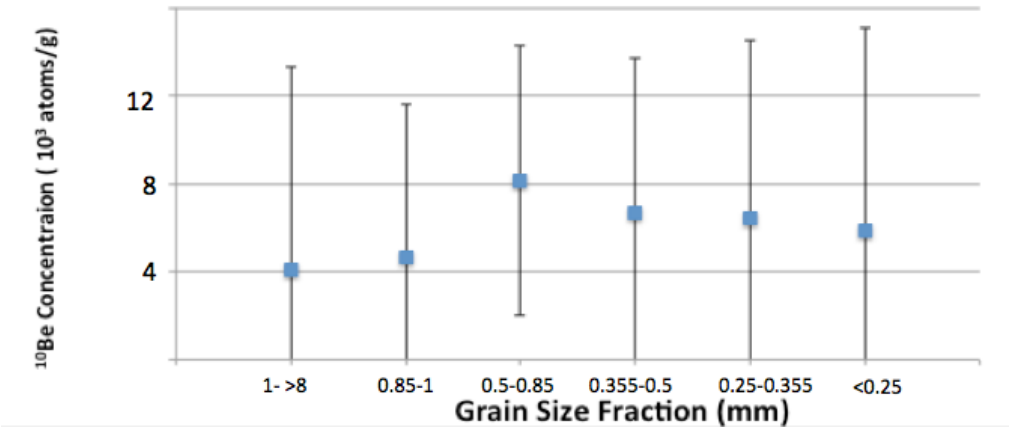


**Figure 12**: Calculated $^{10}Be$ concentrations for samples of different grain sizes.

As well, due to the low measured values and the large errors, none of the values can be statistically distinguished from on another. This being the case, these values give nowhere near enough spread to define a line on an isochron plot.

Considering the $^{26}Al$ data we can see a trend of decreasing $^{26}Al$ concentration with increasing grain size between samples TAME0.150 to TAME0.5-0.85 (Fig 13) (Note that the values on the Y-axis in Figure 13 are an order of magnitude larger than those in Figure 12). This trend is very similar to the trend observed outside the Andes, with lower concentrations in larger grain sizes due to the incorporation of less weathered material during landsliding (discussed earlier). They also compare well with data from the Cordillera Principal in the tectonically-active southern Central Andes (Fig. 5).

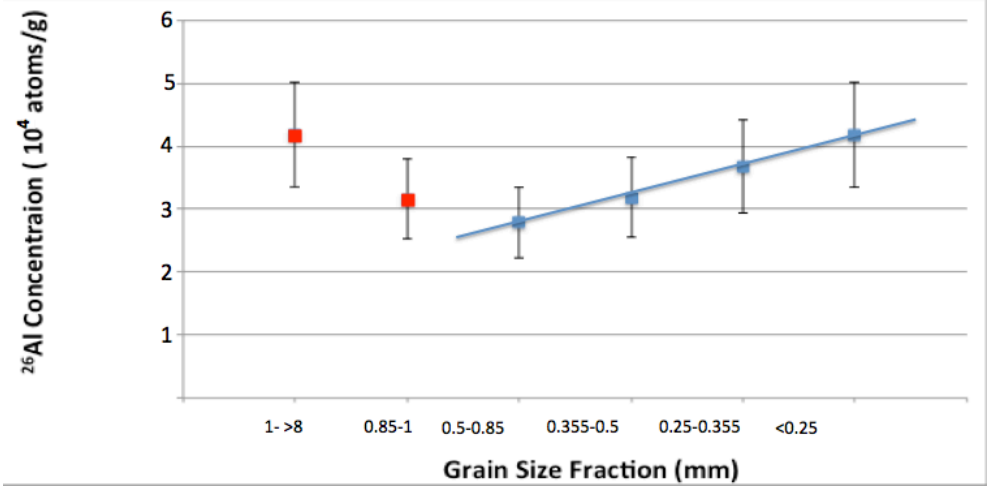


**Figure 13**: Calculated $^{26}Al$ concentrations for samples of different grain sizes.

The two coarsest sand fractions do not fall on this trend line. It is possible to attribute the deviation of these two samples to a statistical issue. When the processing of the samples began, a set mass of 500g for each grain size fraction was used. For the finer grain sizes, several million individual grains were needed to make up this mass. However for the coarser grain size fractions, only a few thousand clasts were needed to get the necessary mass. Each single clast has a unique history of exposure, transport and burial, which will alter its concentration

of cosmogenic nuclides. As a general rule of statistics, the more samples taken, the higher the likelihood the average value reflects the true average for the population. This concept works for sediments (Repka et al., 1997). The larger grain size fractions have less clasts, so there is a greater likelihood that the concentration that they give deviates from the average (Fig. 14).

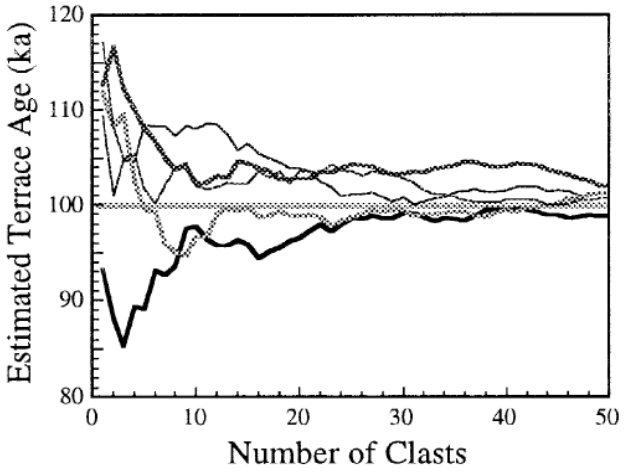


**Figure 14**: Plot of how the age of a terrace, calculated from $^{10}Be$ measurements, can vary depending on the number of clasts sampled. Figure from Repka et al. 1997

5.2 Future work

Though this particular experiment did not work, the methods are more or less correct. Calculating burial ages was very difficult owing to the characteristics of the sample site. If this same project was done in a region with a slower paleo-erosion rate and a younger burial age it is possible that the TCNs would then have high enough concentration in order to resolve a burial age. Therefore, whether an isochron can be developed based on different grain size fractions still remains debatable.

For future work, certain changes to the chemistry will be done. More carrier will be used to ensure that there are enough atoms in the sample to establish a

strong current during AMS measurements. Less quartz will be dissolved for each sample to decrease the amount of unwanted cations entering the columns.

For field techniques, larger grain size fractions should be targeted during sampling to insure enough mass for these grain size fractions is collected. This experiment relied on sand fractions to test if the subtle dependence on grain size was enough to provide the scatter needed to define an isochron. Experiments relying on scatter during the development of depth profiles after deposition prior to burial, or on the possibility that five or more individual cobbles may have sufficient scatter to define an isochron have already been conducted.

This thesis is the second attempt to calculate a burial age for one particular sediment deposit in the Colombian Andes. I believe that it should not be the last. Despite the sample site having a high paleo-erosion rate and an old burial age, it is still a good location for attempting burial dating. It is a very good location to attempt to push the limits of TCN burial dating, and could potentially provide important information about the impact of climatic change on landscape evolution in the Colombian Andes.

As for the grain-size dependent isochron method, I believe that it should be attempted again. The results from this thesis pertaining to the effectiveness of this method are inconclusive. However the amount of evidence showing TCN concentration dependence with grain size in regions of high relief, paired with how useful this method could be in areas where there are no paleosols and no cobbles warrants further testing of the grain-size dependent isochron method.

## 6.0 Conclusion

In conclusion, the effectiveness of a grain-size dependent isochron method has proven inconclusive. The collected samples gave measured concentrations for $^{26}Al$ that ranged from 2.79 to 4.19 X $10^4$ atoms/g (±21% 1-sigma) and for $^{10}Be$ from 4.08 to 8.14 X $10^3$ (±4-8% 1-sigma). These measured values were too low and had too little resolution to be able to define an isochron, meaning that effectiveness of the grain-size dependent isochron method could not be tested.

The reason for these low measured values can most likely be attributed to high erosion rates in the catchment area, resulting in low initial concentrations of TCN in the samples. $^{26}Al$ and $^{10}Be$ may have also been lost during certain steps of the chemical processing since extra quartz mass was dissolved and extra purification steps were needed.

With the collected data, paleo-erosion rates were calculated for the catchment, with $^{10}Be$ giving an erosion rate of 2.59 mm $yr^{-1}$ (±25% 1-sigma) and $^{26}Al$ 0.97 mm $yr^{-1}$ (±33% 1-sigma). These rates suggest that the catchment area was undergoing rapid erosion, at a rate equivalent to other tectonically active orogens.

## 7.0 Reference list

Antinao J. L. (2008). Quaternary Landscape Evolution of the Southern Central Andes of Chile Quantified Using Landslide Inventories, $^{10}$Be and $^{36}$Cl Cosmogenic Isotopes and (U-Th)/He Thermochronology (Doctorial thesis). Retrieved from Dalhousie University.

Balco, G., & Rovey, C. (2008). An isochron method for cosmogenic-nuclide dating of buried soils and sediments. American Journal of Science, 308 (10), 1083-1114.

Balco, G., Rovey, C. (2010). Absolute chronology for major Pleistocene advances of the Laurentide Ice Sheet. Geology, 38(9), 795-798.

Balco, G., Soreghan, G. S., Sweet, D. E., Marra, K. R., & Bierman, P. R. (2013). Cosmogenic-nuclide burial ages for Pleistocene sedimentary fill in Unaweep Canyon, Colorado, USA. Quaternary Geochronology, 18, 149-157.

Belmont, P., Pazzaglia, F.J., & Gosse, J. (2007). Cosmogenic 10Be as a tracer for hillslope and channel sediment dynamics in the Clearwater River, western Washington State. Earth and Planetary Science Letters, 264 (1-2), 123-135.

Cortes M., Angelier, J., Colletta, B. (2006). Structure and tectonics of the central segment of the Eastern Cordillera of Colombia. Journal of South American Earth Sciences, 21 (4), 437-465.

Clapp, E. M., Bierman, P. R., & Caffee, M. (2002). Using 10 Be and 26 Al to determine sediment generation rates and identify sediment source areas in an arid region drainage basin. Geomorphology, 45(1), 89-104.

Clapp, E. M., Bierman, P. R., Nichols, K. K., Pavich, M., & Caffee, M. (2001). Rates of sediment supply to arroyos from upland erosion determined using in situ produced cosmogenic 10 Be and 26 Al. Quaternary Research, 55(2), 235-245.

Clapp, E. M., Bierman, P. R., Schick, A. P., Lekach, J., Enzel, Y., & Caffee, M. (2000). Sediment yield exceeds sediment production in arid region drainage basins. Geology, 28(11), 995-998.

Cyr, A. J., & Granger, D. E. (2008). Dynamic equilibrium among erosion, river incision, and coastal uplift in the northern and central Apennines, Italy. Geology, 36(2), 103-106.

Cyr, A. J., Granger, D. E., Olivetti, V., & Molin, P. (2010). Quantifying rock uplift rates using channel steepness and cosmogenic nuclide–determined erosion rates: Examples from northern and southern Italy. Lithosphere, 2(3), 188-198.

Dingd, L., Liud, T., Donga, W., Caffeee, M. W., & Jullf, A. J. T. (2003). Erosion history of the Tibetan Plateau since the last interglacial: constraints from the first studies of cosmogenic 10Be from Tibetan bedrock. Earth and Planetary Science Letters, 217(33), 33-42.

Gibbard, P. L., Head, M. J., & Walker, M. J. (2010). Formal ratification of the Quaternary System/Period and the Pleistocene Series/Epoch with a base at 2.58 Ma. Journal of Quaternary Science, 25(2), 96-102.

Gosse, J., & Phillips F. M. (2001). Terrestrial in situ cosmogenic nuclides: theory and application. Quaternary Science Reviews, 20, 1474-1560.

Granger, D.E., & Muzikarb, P. F. (2001). Dating sediment burial with in situ-produced cosmogenic nuclides: theory, techniques, and limitations. Earth and Planetary Science Letters, 188, 269-281.

Granger, D. E., Riebe, C. S., Kirchner, J. W., & Finkel, R. C. (2001). Modulation of erosion on steep granitic slopes by boulder armoring, as revealed by cosmogenic 26 Al and 10 Be. Earth and Planetary Science Letters, 186(2), 269-281.

Gregory-Wodzicki K.M. (2000) Uplift History of the Northern and Central Andes: a review. GSA Bulletin, 112 (7), 1091–1105.

Heimsath, A. M., Dietrich, W. E., Nishiizumi, K., & Finkel, R. C. (2001). Stochastic processes of soil production and transport: Erosion rates, topographic variation and cosmogenic nuclides in the Oregon Coast Range. Earth Surface Processes and Landforms, 26(5), 531-552.

Heimsath, A. M., Chappell, J., Dietrich, W. E., Nishiizumi, K., & Finkel, R. C. (2000). Soil production on a retreating escarpment in southeastern Australia. Geology, 28(9), 787-790.

Hidy, H. J. (2013). Cosmogenic Nuclide Quantification of Paleo-Fluvial Sedimentation Rates in Response to Climate Change (Doctorial dissertation). Retrieved from Dalhousie University.

Hidy, A. J., Gosse, J. C., Blum, M. D., & Gibling, M. R. (2014). Glacial–interglacial variation in denudation rates from interior Texas, USA, established with cosmogenic nuclides. Earth and Planetary Science Letters, 390, 209-221.

Hidy, A. J., Gosse, J. C., Pederson, J. L., Mattern, J. P., & Finkel, R. C. (2010). A geologically constrained Monte Carlo approach to modeling exposure ages from profiles of cosmogenic nuclides: An example from Lees Ferry, Arizona. Geochemistry, Geophysics, Geosystems, 11(9).
Chicago

Kohl, C. P., & Nishiizumi, K. (1992). Chemical isolation of quartz for measurement of in-situ -produced cosmogenic nuclides. Geochimica et Comochimica Acta. 56, 3583-3587.

Lal, D. (1991). Cosmic ray labeling of erosion surfaces: in situ nuclide production rates and erosion models. Earth and Planetary Science Letters, 104(2), 424-439.

Parra M., Mora, A., Jaramillo, C., Torres, V., Zeilinger G., & Strecker M. R. (2010) Tectonic controls on Cenozoic foreland basin development in the north-eastern Andes, Colombia. Basin Research, 22, 874–903.

Puchol N., LavlZ' , J., Lupker, M., Blard, P-H., Gallo, F., France Lanord, C., & ASTER Team. (2014). Grain-size dependent concentration of cosmogenic 10Be and erosion dynamics in a landslide-dominated Himalayan watershed. Geomorpholgy, 224, 55-68.

Rees-Jones, J. (1995). Optical dating of young sediments using fine-grain quartz. Ancient TL, 13(2), 9-14.

Repka J. L., Anderson R. S., & Finkel R. C. (1997). Cosmogenic dating of fluvial terraces, Fremont River, Utah. Earth and Planetary Science Letters. 152, 59-73.

Rybczynski, N., Gosse, J. C., Harington, C. R., Wogelius, R. A., Hidy, A. J., & Buckley, M. (2013). Mid-Pliocene warm-period deposits in the High Arctic yield insight into camel evolution. Nature communications, 4, 1550.

Schaller, M., Von Blanckenburg, F., Veldkamp, A., Tebbens, L. A., Hovius, N., & Kubik, P. W. (2002). A 30 000 yr record of erosion rates from cosmogenic 10 Be in Middle European river terraces. *Earth and Planetary Science Letters*, *204*(1), 307-320.

Stock, G. M., Frankel, K. L., Ehlers, T. A., Schaller, M., Briggs, S. M., & Finkel, R. C. (2009). Spatial and temporal variations in denudation of the Wasatch Mountains, Utah, USA. Lithosphere, 1(1), 34-40.

Vance, D., Bickle, M., Ivy-Ochs, S., & Kubik, P. W. (2003). Erosion and exhumation in the Himalaya from cosmogenic isotope inventories of river sediments. Earth and Planetary Science Letters, 206(3), 273-288.

Veloza, G., Taylor, M., Mora, A., & Gosse, J. (Unpub). Active mountain building along the eastern Colombian Sub-Andes: A folding history from deformed terraces across the Tame Anticline, Llanos Basin. University of Kansas, Lawrence KS.

Veloza Fajardo, G. E. (2012). *Active faulting and Quaternary slip rates of the Colombian sub-Andes* (Doctoral dissertation, University of Kansas).